

The structure of the pleiotropic transcription regulator CodY provides insight into its GTP-sensing mechanism

Ah-reum Han¹, Hye-Ri Kang¹, Jonghyeon Son¹, Do Hoon Kwon², Sulhee Kim¹, Woo Cheol Lee¹, Hyun Kyu Song², Moon Jung Song¹ and Kwang Yeon Hwang^{1,*}

¹Department of Biosystems & Biotechnology, Korea University, Anam-dong, Seoungbuk-gu, Seoul 136-713, South Korea and ²Department of Life Sciences, College of Life Sciences & Biotechnology, Korea University, Anam-dong, Seoungbuk-gu, Seoul 136-713, South Korea

Received April 09, 2016; Revised August 21, 2016; Accepted August 24, 2016

ABSTRACT

GTP and branched-chain amino acids (BCAAs) are metabolic sensors that are indispensable for the determination of the metabolic status of cells. However, their molecular sensing mechanism remains unclear. CodY is a unique global transcription regulator that recognizes GTP and BCAAs as specific signals and affects expression of more than 100 genes associated with metabolism. Herein, we report the first crystal structures of the full-length CodY complex with sensing molecules and describe their functional states. We observed two different oligomeric states of CodY: a dimeric complex of CodY from *Staphylococcus aureus* with the two metabolites GTP and isoleucine, and a tetrameric form (apo) of CodY from *Bacillus cereus*. Notably, the tetrameric state shows in an auto-inhibitory manner by blocking the GTP-binding site, whereas the binding sites of GTP and isoleucine are clearly visible in the dimeric state. The GTP is located at a hinge site between the long helical region and the metabolite-binding site. Together, data from structural and electrophoretic mobility shift assay analyses improve understanding of how CodY senses GTP and operates as a DNA-binding protein and a pleiotropic transcription regulator.

INTRODUCTION

Global regulators are protein factors that control many genes and operons, thereby coordinating nutrient flow in response to a small number of specific metabolite signals. Through these regulators, bacteria can manage their over-

all metabolite status (1,2). Amino acids or nucleotides are also used as signal molecules in monitoring of intracellular energy pools and carbon sources (3–5). In particular, GTP is an important signaling molecule, owing to its association with amino acid limitation, and it induces a bacterial response to harsh environments (6,7).

CodY, a pleiotropic transcription factor that is highly conserved in low-G+C Gram-positive bacteria, controls the expression of >100 genes involved in intracellular metabolic responses to environmental growth conditions (1,8–14). It is a unique regulator because it uses both amino acids and GTP as sensing metabolites (10). The activity of CodY, a DNA-binding protein, is enhanced by interaction with GTP and branched-chain amino acids [BCAAs; leucine, isoleucine, and valine (ILV)] in *Bacillus subtilis*, *Clostridium difficile*, *Listeria monocytogenes*, and *Staphylococcus aureus* (15–20). Interestingly, CodY from *Lactococcus lactis* and *Streptococcus pneumoniae* respond to BCAA but not to GTP (21,22). CodY activity is influenced by the intracellular concentrations of these effectors (23–26). The consensus sequence of the CodY-binding site is AATTTTCW-GAAAATT (27–29).

Structures of CodY fragments have been reported for the isoleucine-bound N-terminal metabolite-binding domain (MBD) and the C-terminal DNA-binding domain (DBD) from *Bacillus subtilis* (30). Structural changes in the MBD caused by interactions with BCAAs systemically affect the DNA-binding activity of CodY (24). The GTP-binding site is not anticipated to be located in the ligand or MBD, and three conserved motifs in CodY homologues, found in small GTPase proteins, are expected to be involved in GTP binding (15,17,24,30). However, the actual GTP-binding site of CodY remains unknown.

To understand the GTP-sensing mechanism of CodY, we determined the first crystal structures of full-length CodY from *Staphylococcus aureus*, in complex with GTP and

*To whom correspondence should be addressed. Tel: +82 2 3290 3512; Fax: +82 2 923 3229; Email: chahong@korea.ac.kr
Present address: Kwang Yeon Hwang, Department of Biosystems & Biotechnology, College of Life Sciences & Biotechnology, Korea University, Anam-dong, Seoungbuk-gu, Seoul 136-713, South Korea.

isoleucine (Ile) (*saCodY*), and from *Bacillus cereus* (apo-*bcCodY*). Our structures reveal two different oligomeric states: a dimer (*saCodY*) and a tetramer (*bcCodY*). Unexpectedly, the DNA-binding motif and GTP-binding site of tetrameric CodY are mutually obstructed. The two states reflect the inactive state (*bcCodY*) under insufficient nutrient conditions and the active state (*saCodY*) under conditions in which energy sources are sufficient. Moreover, there is no difference in the MBD after GTP binding, but the helical linker is bent slightly by approximately 15 degrees, thereby moving the position of the DBD in the dimeric CodY. The active state enhances DNA-binding activity when nutrients are abundant, and the inactive state blocks DNA binding under low-nutrient conditions. Our findings allow understanding of the role of GTP in the DNA-binding activity of CodY and demonstrate how CodY senses GTP and pleiotropically operates as a DNA-binding protein.

MATERIALS AND METHODS

Cloning, protein expression, and purification of recombinant *saCodY* and *bcCodY*

The full-length *CodY* gene encoding *saCodY* (SWISS-PROT entry: A7×1N2, residues 1–257) and *bcCodY* (Q819×8, residues 1–259) was amplified by PCR and cloned into pET28a. The recombinant protein with an N-terminal His-tag was expressed in *Escherichia coli* strain BL21 (DE3) at 18°C for 16 h. The SeMet derivative of *bcCodY* was prepared in *E. coli* B834 cells. The expressed CodY proteins (*saCodY* and *bcCodY*) were purified by nickel-affinity chromatography (GE Healthcare, Seoul, South Korea) in buffer containing 50 mM Tris (pH 8.0), 100 mM NaCl, and 2 mM β-mercaptoethanol. The proteins were eluted with a linear gradient of imidazole (5–500 mM). The collected proteins were further purified by gel-filtration chromatography (Superdex-75; GE Healthcare) in buffer containing 50 mM Tris (pH 8.0), 100 mM NaCl, and 5 mM DTT. The collected proteins were concentrated to 10 mg ml⁻¹ using Centricon concentrators (Merck Millipore, Seoul, South Korea) and stored at -70°C before use. The mutants *saCodY* (E153A and 3P5A) and *bcCodY* (R167AE183AE252A) were over-expressed and purified by the same protocol.

Crystallization and data collection

Crystals of *bcCodY* (SeMet) were grown by the hanging-drop vapor-diffusion method at 20°C with crystallization buffer containing 100 mM Tris (pH 8.5), 200 mM MgCl₂, and 20% PEG400. *saCodY* protein was incubated with 2 mM GTP and 10 mM Ile for 30 min at 4°C for co-crystallization and was then crystallized. *saCodY* crystals were grown in buffer composed of (i) 0.2 M ammonium acetate, 0.1 M sodium citrate dehydrate (pH 5.9), and 26% PEG400 and (ii) 10% (v/v) 2-propanol, 0.1 M tri-sodium citrate (pH 5.0) and 26% PEG400. Diffraction data were collected at the Pohang Accelerator Light Source beamline 5C (Pohang, South Korea) and the Photon Factory beamline BL1A (Tsukuba, Japan). All collected images were processed and scaled with the HKL-2000 package (31).

Structure determination and refinement

The *saCodY* crystal complexed with GTP and Ile [*saCodY* (I) and *saCodY* (II)] belonged to orthorhombic space group *P*2₁2₁2₁ with unit cell dimensions *a* = 45.89 Å, *b* = 76.03 Å, *c* = 158.02 Å and *saCodY* (II) with unit cell dimensions *a* = 45.82 Å, *b* = 75.99 Å, *c* = 166.30 Å. The asymmetric unit contained two molecules (Supplementary Figure S1C). The initial structure of *saCodY* (I) was solved by molecular replacement with MOLREP (32), using partial models (PDB entry: 2B0L and 2B18) as a search model in the CCP4 suite (33). The second structure of *saCodY* (II) was obtained from PHASER (34) in PHENIX (35) by using the first *saCodY* (I) structure as a search model. The crystal of *bcCodY* (SeMet) belonged to hexagonal space group *P*6₁ with unit cell dimensions *a* = *b* = 131.85 Å, *c* = 224.02 Å, and the asymmetric unit contained four molecules (Supplementary Figure S1D). The initial phases for *bcCodY* were obtained from single-wavelength anomalous dispersion (SAD). Selenium sites were located using the AutoSol (36) module in PHENIX. Model building was performed automatically with the AutoBuild (37) module in PHENIX and manually with COOT (38). The final model refinement was performed in Refmac (39). The final models were validated using MolProbity (40) and had R values of *saCodY* (I) with *R*_{cryst} = 17.75%/*R*_{free} = 20.92%, *saCodY* (II) with *R*_{cryst} = 18.42%/*R*_{free} = 23.01%, and *bcCodY* (SeMet) with *R*_{cryst} = 23.78%/*R*_{free} = 27.73%. The data collection and structure refinement statistics are summarized in Table 1. All structure figures were generated in PyMOL (DeLano Scientific LLC). The structure factor and coordinate files have been deposited in the Protein Data Bank under accession codes 5EY0, 5EY1 and 5EY2.

Size-exclusion chromatography

To confirm the oligomeric state, 100 μM purified *bcCodY* and *saCodY* were reloaded onto a gel-filtration column (Superdex 200 10/300 GL, GE Healthcare) in buffer A containing 50 mM Tris (pH 8.0), 100 mM NaCl, and 2 mM DTT. After incubation with 1 mM GTP for 30 min, *bcCodY* and *saCodY* were loaded onto the gel-filtration column in buffer A with 1 mM GTP to minimize the effect of GTP loss during electrophoresis. Ile was not added to any sample or buffer. The same experiments were performed in a buffer A with 1 mM Ile. The mutant *saCodY* and *bcCodY* proteins were examined through the same protocol.

Electrophoretic mobility shift assays

The purified wild-type and mutant *saCodY* proteins (0–48 μM) were incubated with ³²P-labeled 45-mer dsDNA (35 nM) in a buffer containing 25 mM Tris (pH 8.0), 25 mM KCl, 2.5 mM MgCl₂, 2.5% glycerol, 100 ng of BSA, 50 ng of poly (dI-dC) and 0.25 mM EDTA. Ile was not added to any sample or buffer. After incubation at RT for 30 min, electrophoresis was carried out for 60 min in 0.5X TBE buffer at 100 V. For some reactions involving GTP, 1× TBE buffer was supplemented with 2 mM GTP. All gels were exposed to a phosphorimager screen and visualized with laser scanner Typhoon FLA 7000 and software. Quantification of the bound and unbound dsDNA fraction to calculate *K*_d values

Table 1. Data collection and refinement statistics

	saCodY (I)	saCodY (II)	bcCodY (SeMet)
Data collection			
Space group	<i>P</i> 2 ₁ 2 ₁ 2 ₁	<i>P</i> 2 ₁ 2 ₁ 2 ₁	<i>P</i> 6 ₁
Cell dimensions			
a, b, c (Å)	45.89, 76.03, 158.02	45.82, 75.99, 166.30	132.01, 132.01, 223.082
α, β, γ (°)	90, 90, 90	90, 90, 90	90, 90, 120
			<i>Peak</i>
Wavelength (Å)	1.0000	1.0000	0.97921
Resolution (Å)	30.0-1.60	30.0-2.0	30.0 - 3.0
(outer shell)	(1.63-1.60)	(2.04-2.00)	(3.08-3.00)
FOM			0.470
<i>R</i> _{merge} (%) ^b	7.2 (31.3) ^a	8.6 (34.1)	10.9 (47.5)
<i>I</i> /σ	23.72 (2.17)	17.03 (2.16)	16.83 (3.08)
Completeness (%)	94.3 (92.8)	98.4 (92.4)	99.9 (99.9)
Redundancy	3.9 (2.8)	5.3 (3.2)	12.1 (6.5)
Refinement			
Resolution (Å)	30.0 - 1.6	30 - 2.0	30.0-3.0
No. of Reflections	69602	41162	43902
<i>R</i> _{work} / <i>R</i> _{free} (%) ^c	17.75/20.92	18.42/23.01	23.78/27.73
Average <i>B</i> -factor (Å ²)	36.60	38.10	64.30
Root-mean-square-deviations			
Bond length (Å)	0.0069	0.0080	0.0043
Bond angle (°)	1.076	1.165	1.005
Ramachandran favored (%)	97.2	97.7	91.2
Ramachandran outliers (%)	0.2	0.3	0.7
PDB entry	5EY0	5EY1	5EY2

^aValues in parentheses refer to the highest resolution shell.

^b $R_{merge} = \frac{\sum_{hkl} \sum_i |I_{hkl} - \langle I_{hkl} \rangle|}{\sum_{hkl} \sum_i I_{hkl}}$

^c $R_{cryst} = \frac{\sum_{hkl} ||F_o| - |F_c||}{\sum |F_o|}$

was performed with ImageJ. A nonlinear regression curve was fitted using GraphPad Prism software.

RESULTS

Overall structure of CodY

The crystal structure of *saCodY* (I) at a resolution of 1.6 Å was determined by molecular replacement. Two molecules were contained in the asymmetric unit (Supplementary Figure S1C). Each monomeric structure exhibits a striking dumbbell-shaped molecule, in which the GAF domain—the MBD in the N-terminal—and the winged helix-turn-helix (wHTH) domain—the DBD in the C-terminal—are con-

nected by a ~61-Å-long helical linker (LHL) composed of >41 amino acids (residues 137–178; Figure 1A). We also detected clear electron density of GTP molecules at the interface between the MBD and LHL (Figure 1A and C). The other metabolite cofactor (Ile) is also bound to the MBD (Figure 1A). The dimeric structure shows the same dumbbell shape with a direction parallel to the LHL, and the dimer interface of the MBD is composed of highly conserved residues found across CodY homologs (30). Whereas the MBD shows a two-fold symmetry in the dimeric structure, the DBD is slightly twisted, owing to the absence of DNA. In the case of *saCodY* (II), one of these DBDs is not shown, because of its flexibility and disorder (Supplementary Figure S1A and B). We solved the tetrameric conformation of *bcCodY* in an unbound state, unlike the solution of the dimeric structure of *saCodY*, which is bound to metabolites (Figure 1B and Supplementary Figure S1D). Two protomers (molA and molB) of *bcCodY* consist of two functional domains (MBD and DBD) and an LHL similar to that of *saCodY*. In the case of molC and molD, the MBD is partially disordered (residues 22–23, 64–65, 91–106 and 120–123 in molC, and residues 1–3, 60–64, 92–108 and 119–123 in molD) (Figure 1B). Overall, each MBD faces the opposite side and crosses the DBDs (Figure 1B), and four DBDs assemble at the center of the tetrameric *bcCodY* (Supplementary Figure S2). Four LHLs and each DBD are involved in the tetramerization (Figure 2A–C). There are two interfaces between molC and the dimer of molA and molB. In detail, S177 in the LHL and E252 in the DBD of molA interact with R167 in the LHL and K255 in the DBD of molC, respectively (Figure 2B). A second interface is present between the middle of the LHL in molB and the distal portion of the LHL and DBD in molC. R167 and M174 in the LHL of molB form hydrogen bonds with S177, M174 and R167 of molC (Figure 2C). In addition, the MBD of molB interacts with molC through hydrogen bonds between K20 of molB and E183 of molC (Figure 2C). The same interactions were observed between molD and the dimer of molA and molB. They have a root-mean-square deviation (RMSD) value of approximately 0.204 Å over 122 Cα (residues 1–136) of the MBD, 0.517 Å over 69 Cα (residues 179–257) of the DBD between the four protomers in *bcCodY*, 0.262 Å over 123 Cα (residues 1–136) of the MBD, and 1.225 Å over 71 Cα (residues 179–255) of the DBD between the two protomers in *saCodY* (Figure 1). Size-exclusion chromatography indicated that *saCodY* and *bcCodY* are tetramers (~130 kDa), but they eluted in a broad range of volumes covering tetramers to dimers. However, the triple mutant of *bcCodY* (R167A, E183A and E252A), affecting the tetrameric interface, eluted in a volume indicating a dimer (Figure 2E). It was reported a dimer-tetramer distribution that was monodispersed to dimer by GTP (41). Therefore, after incubation of *saCodY* and *bcCodY* with GTP, the proteins eluted at much smaller sizes than those of *saCodY* and *bcCodY* alone (Figure 2F and G). However, their oligomeric states were not changed by addition of Ile (Supplementary Figure S3A and B). The four side chains, A207, D208, R214 and S215, positioned in the HTH motif of the DBD, are essential for the DNA-binding activity of CodY (42). This region is clearly blocked by the MBD of other protomers in the *bcCodY* structure

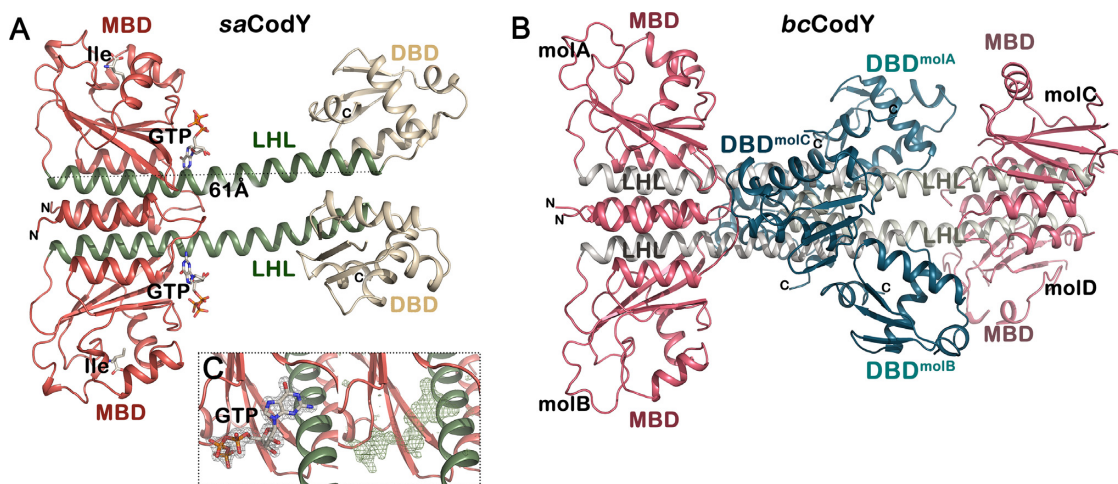


Figure 1. Overall structure of *saCodY* and *bcCodY*. (A) Ribbon diagram of the overall structure of *saCodY*. The metabolite-binding domain (MBD), long helical linker (LHL) and DNA-binding domain (DBD) are colored as bright red, green, and wheat, respectively. GTP and Ile are displayed as a stick model. The dashed line indicates the length of the LHL with 61 Å. (B) Overall structure of *bcCodY*. Each monomer is labeled as molA, molB, molC and molD. The MBD and LHL are colored as pink and gray, respectively. The DBD of molA and molB and the DBD of molC and molD are colored as light teal and deep teal, respectively. (C) Close-up view of GTP of *saCodY* with the $2F_o - F_c$ electron density map at 1.0σ (left) and unbiased $F_o - F_c$ electron density map at 3.0σ (right) from the simulated annealing omit map.

(Figure 2D). The HTH motif of the DBD (residues 203–227) is closely packed against the MBD of the molecule on the opposite side. The distance is ~ 5.5 – 8.4 Å, thus indicating that *dsDNA* binding is not possible (Figure 2D). Thus, our results suggest that the tetrameric *bcCodY* structure is the inactive form, blocking DNA-binding activity, whereas the dimeric *saCodY* complex with two metabolites is the intermediate state, which is ready to be activated, thus allowing DNA binding.

Two metabolite-binding sites in *saCodY*

The *saCodY* structures co-crystallized with two metabolites, Ile and GTP, show a dimeric state (Figure 1A). Two Ile molecules are enclosed in a pocket formed above the β -sheet of the MBD in each protomer. The binding site of Ile is similar to that of *bsCodY* (CodY from *Bacillus subtilis*) (24). In detail, R61 forms salt bridges with the carboxylate group of Ile and E101. The oxygen of T96 is hydrogen-bonded to the amino group of Ile (Supplementary Figure S4A). Studies have been performed to identify the putative GTP-binding site; however, unlike the Ile-binding site, the identity of the GTP-binding site remains unknown. A comparison of the putative GTP-binding motifs in the CodY homologs with small GTPases has predicted that three highly conserved motifs, G1 (GXXXXGXT), G3 (DXXG) and G4 (NKXD), are involved in GTP binding (15,17). However, GTP is positioned in an entirely different site in our *saCodY* structure. Surprisingly, two GTP molecules are located in the middle of the entire dimeric structure, unlike Ile. A GTP is positioned in the space between the MBD and LHL, thus suggesting that the residues associated with GTP binding are located in the MBD and LHL (Figure 3A). Structural comparison shows that the GTP-binding site of *saCodY* is not located in the GAF domain of the MBD (Supplementary Figure S4B) (17,24,30). Six residues (V22, F24, S43, R45, K47 and H70) interact with the GTP molecule in the

MBD. V22 and F24 are located in motif 1 (the loop between $\alpha 1$ and $\alpha 2$). Three residues, S43, R45 and K47, are in motif 2 (the region between $\beta 1$ and $\beta 2$), and H70 is in motif 3 (the region between $\alpha 4$ and $\alpha 5$). The two residues E153 and K158 are also important in the interaction with GTP and are located in the LHL. These eight residues tightly interact with GTP along with two well-ordered water molecules (Figure 3B). However, these residues are not conserved but are included in a similar group across the CodY homologs (Figure 3C). The purine ring of GTP inserts into a pocket formed between the GAF domain of the MBD and LHL (Figure 3A). We divided the GTP-binding site into two parts: the phosphate-binding site (P-pocket) and the guanosine-binding site (G-pocket; Figure 3A). In competition assays, GTP and ATP, but not UTP or CTP, binds to CodY, and GTP has a higher affinity than ATP to CodY (15). The structural difference between GTP and ATP is the presence of the amino group at C-2 in the guanine as the hydrogen-bond donor in GTP, and the replacement O-6 in guanine with N-6 in adenine. In the G-pocket of *saCodY*, the O-6 atom is hydrogen-bonded with the main-chain amino acid group of F24. Additionally, the O ϵ atom of E153 is hydrogen-bonded with this amino group. These two hydrogen-bond interactions may explain the difference between binding GTP and ATP for CodY. The carbonyl group of the main chain in V22 also interacts with N-1 in guanine via a hydrogen bond. F24 is involved in structural stability via a π - π hydrophobic interaction between the benzene ring of F24 and the purine ring of GTP. The P-pocket is formed with the GAF domain and helix $\alpha 7$. S43, R45, K47, and H70 of motifs 1 and 2 and K158 of LHL interact with the three phosphates with two water molecules via hydrogen bonds (Figure 3B). CodY recognizes GTP as a metabolite without hydrolysis (15). There was no metal ion, such as magnesium, to serve as the electron donor for GTP-hydrolysis. Moreover, CodY can be activated by non-hydrolyzable analogs of GTP (17). In summary, these

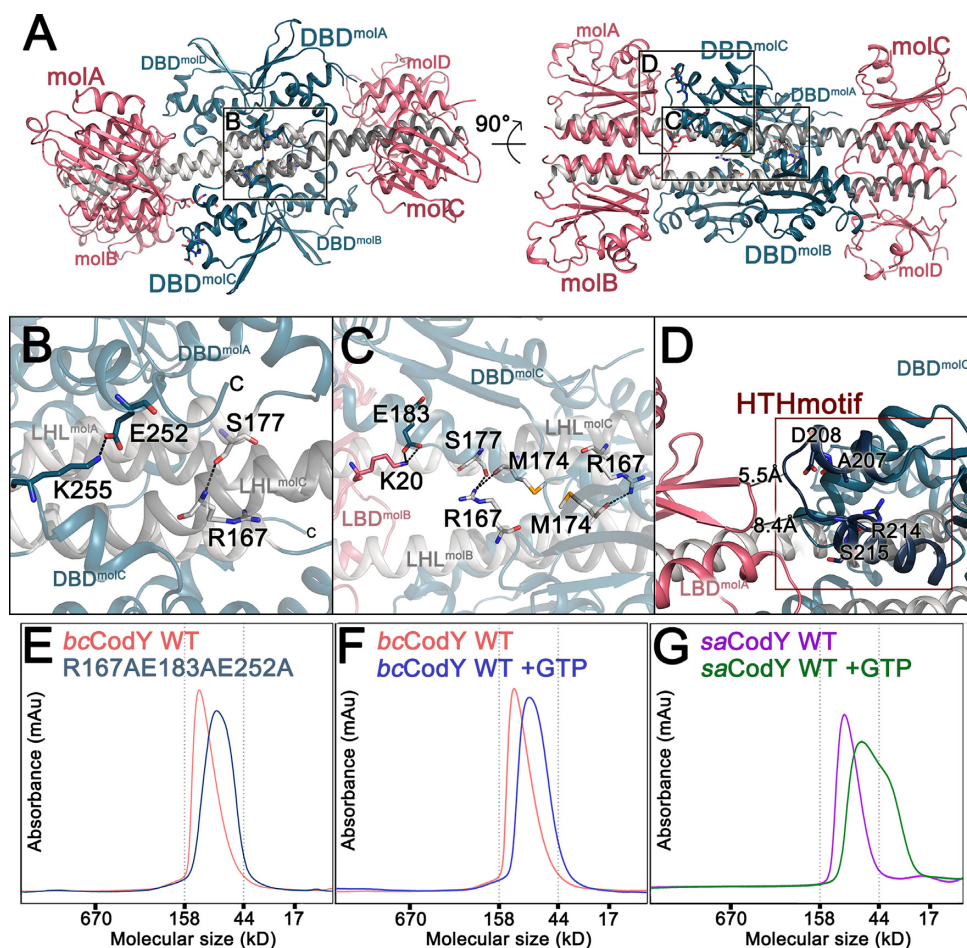


Figure 2. Tetramer state of CodY. Representative interactions between four molecules of *bcCodY* (molA–molD). (A) The overall tetrameric *bcCodY* structure in two orientations. Each domain is colored as in Figure 1B. Black-lined squares indicate tetrameric interface (2B and 2C) and HTH motif (2D). (B and C) Close up view of tetrameric interface. The residues involved in the interactions are represented as stick models. The dashed lines indicate hydrogen bonds. (D) Interface of the HTH motif blocked by the tetramer formation. Four essential residues, A207, D208, R214, and S215, for DNA binding are shown as stick models. The red line square indicates the HTH motif in the DBD. The closest (5.5 Å) and longest (8.4 Å) distances between the HTH motif of molC and the MBD of molA are measured. (E–G) Changes in oligomeric states of CodY proteins determined by size-exclusion chromatography. (E) Elution profiles of *bcCodY* WT (light pink) and *bcCodY* R167AE183AE252A (deep blue). (F) Elution profiles of *bcCodY* WT (light pink) and *bcCodY* WT with GTP (blue). (G) Elution profiles of *saCodY* WT (purple) and *saCodY* WT with GTP (green).

GTP-binding pockets in the *saCodY* structure indicate that CodY may not be involved in GTP hydrolysis.

Implications for DNA binding activity of CodY in the presence of GTP

According to a report on the interaction between CodY and GTP, the purine ring and the γ phosphate of GTP are both important in the activation of CodY (15,17). To determine whether there is a direct interaction between CodY and GTP, we performed surface plasmon resonance (SPR) analysis with GTP, ATP, GDP, or GMP. The results showed that GTP had the highest binding affinity and that the binding affinities of GDP, GMP and ATP were 10 times lower than that of GTP to *saCodY* (Table 2, see also Supplementary Figure S5). To confirm the binding site of *saCodY*, we performed additional SPR analysis using several mutants that interacted with GTP. In the E153A mutant, residue E153 in the G-pocket, relevant to GTP selectivity, was replaced with Ala. The mutant 3P5A contained five residues related

to the P-pocket, S43, R45, K47, H70 and K158, which were mutated to Ala. The SPR analysis showed that E153A and 3P5A had a lower GTP-binding affinity than that of wild-type *saCodY* (Table 2, see also Supplementary Figures S5 and S6). However, the oligomeric states of mutants were not changed by GTP (Supplementary Figure S3C–D).

The DNA-binding activity of CodY is enhanced by the binding of GTP metabolites and BCAA (15–17). To understand the relationship between DNA-binding affinity and GTP binding in *saCodY*, we carried out electrophoretic mobility shift assays (EMSAs). The EMSAs were performed with wild-type *saCodY* and the mutants-E153A and 3P5A, using 32 P-labeled 45 bp oligonucleotides containing a single CodY-binding sequence from the *ilvB* promoter region (*ilvB*) in either the state containing GTP or that with no GTP (Figure 4 and Supplementary Figure S7). The K_d values of E153A and 3P5A in the presence of GTP were 2.8-fold and 6.5-fold higher, respectively, than that of wild-type *saCodY*; this result shows that the G-pocket and the P-

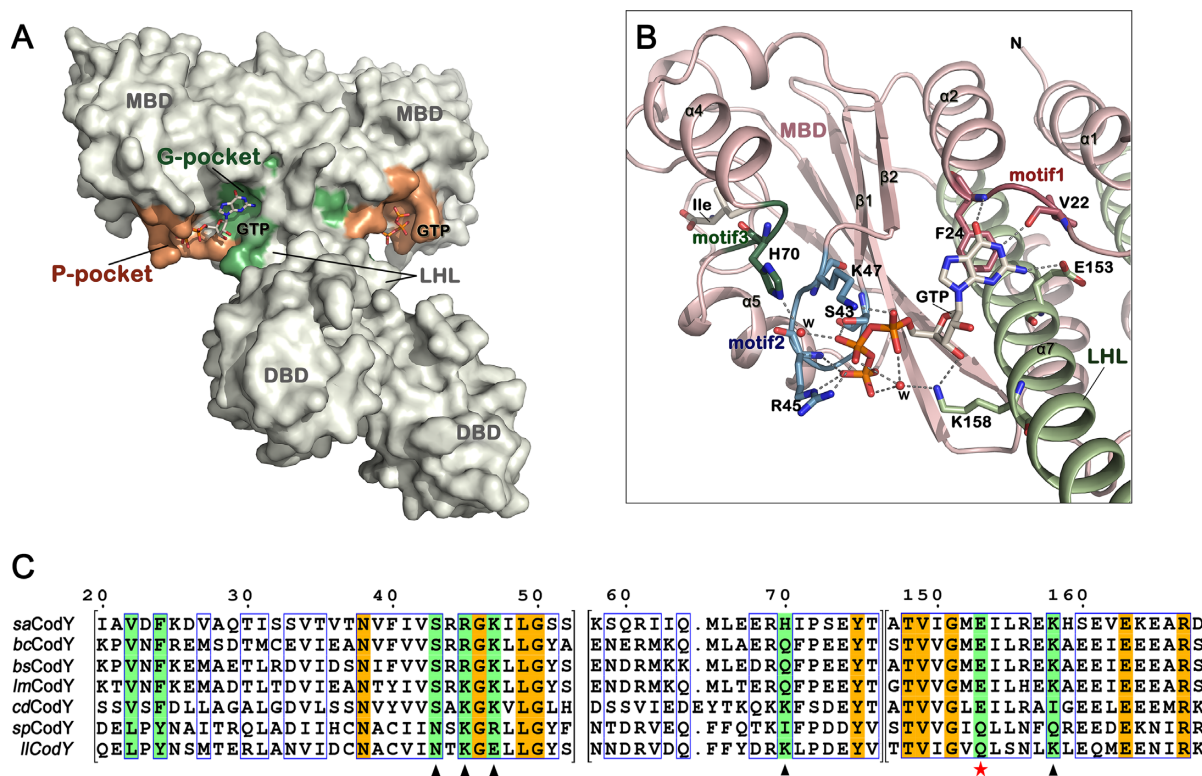


Figure 3. GTP-binding site of *saCodY*. (A) Surface representation of *saCodY* dimer with GTP. The domains of *saCodY* are labeled. Two GTP molecules are located in the space between the MBD and LHL of each protomer. The G-pocket and P-pocket are colored green and orange, respectively. (B) Close-up view of the GTP-binding site. Eight residues associated with GTP binding are shown as stick models. Six residues in three motifs [motif 1 (raspberry): loop between helices $\alpha 1$ and $\alpha 2$, motif 2 (light teal): loop between strands $\beta 1$ and $\beta 2$ and motif 3 (forest): loop between helices $\alpha 4$ and $\alpha 5$] in the LBD and two residues of the LHL participating in the formation of the pockets are displayed. Water molecules labeled 'w' are depicted by a red sphere. The dashed lines represent hydrogen bonds. (C) Partial sequence alignment of the GTP-binding site in CodY analogues from various Gram-positive bacteria. Each sequence is *saCodY* (SWISS-PROT entry: A7 \times 1N2) with *bcCodY* (Q819 \times 8), *bsCodY* (*Bacillus subtilis*, P39779), *lmCodY* (*Listeria monocytogenes*, Q8Y7J7), *cdCodY* (*Clostridium difficile*, U3XTB4), *spCodY* (*Streptococcus pneumoniae*, B2IRA0) and *lICodY* (*Lactococcus lactis*, Q032T5). The orange boxes and blue frames represent strictly conserved residues and residues with similar characteristics, respectively. The light green boxes are relevant to residues associated with GTP binding, a black triangle and a red star indicate residues relevant to P-pocket and G-pocket, respectively.

Table 2. Kinetic analysis of *saCodY*-GTP interactions determined by SPR experiments

Protein	Analyte	k_a ($M^{-1}s^{-1}$)	k_d (s^{-1})	K_d (mM)
<i>saCodY</i> Wild-type	GTP	1.9 (± 0.1)E2	0.43 (± 0.03)	2.26 (± 0.03)
	GDP	13.0 (± 0.3)	0.221 (± 0.006)	17 (± 2)
	GMP	12.0 (± 0.5)	0.245 (± 0.005)	20 (± 1)
	ATP	16.0 (± 0.1)	0.310 (± 0.009)	19 (± 2)
<i>saCodY</i> E153A	GTP	8.3 (± 0.2)	0.233 (± 0.006)	28 (± 3)
<i>saCodY</i> 3P5A	GTP	5.6 (± 0.7)	0.192 (± 0.004)	35 (± 5)

pocket both have an effect and that the P-pocket may be more important than the G-pocket in CodY DNA binding in the presence of GTP (Figure 4). The DNA-binding affinity of the wild type was significantly increased by the addition of GTP (2-fold), but E153A binding was only slightly increased (1.3-fold) and 3P5A binding showed no changes in the presence of GTP compared with the affinities in the absence of GTP, thus indicating that the GTP-binding site, including the G-pocket and P-pocket, is associated with GTP binding and the regulation of the DNA binding of CodY (Figure 4B and Supplementary Figure S7). The γ phosphate of GTP is important for activation of CodY (17). Our data are consistent with these previous findings in that the CodY interaction with the phosphate of GTP

at the P-pocket was critical for the DNA-binding affinity of CodY. The K_d values of E153A and 3P5A were 1.7-fold and 3.0-fold higher than that of the wild-type in the absence of GTP. These data suggest that altering the GTP-binding site of CodY may affect CodY's DNA-binding affinity even in the absence of GTP. This altered affinity may occur because the mutation in the GTP-binding site that leads to oligomeric CodY favors its inactive form, thereby affecting the accessibility of DNA as a substrate. Alternatively, the mutation may affect the stability of the CodY protein dimer, thus resulting in decreased DNA-binding affinity. CodY senses the intracellular GTP concentration as an indicator of nutritional limitations; therefore, at low GTP concentrations, CodY no longer binds GTP, the affinity for DNA is

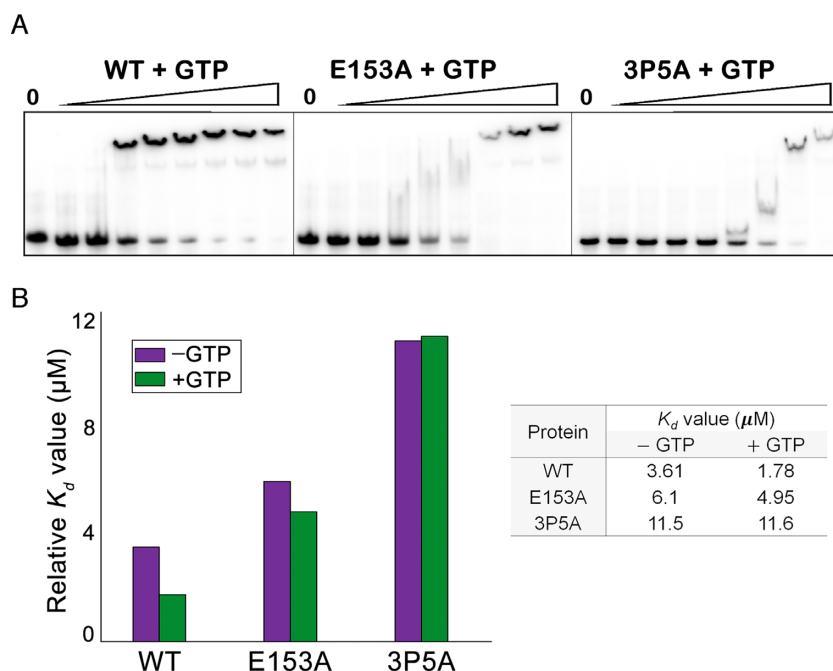


Figure 4. DNA-binding activities of wild-type and mutant *saCodY*. (A) The electrophoretic mobility shift assays of *saCodY* proteins were performed using ^{32}P -labeled 45-mer *dsDNA* (35 nM) containing the *ilvB* promoter region. The wild type, E153A relevant to GTP specificity, and 3P5A relevant to the P-pocket of *saCodY* were incubated with a substrate consisting of DNA and 2 mM GTP. All sets of experiments were conducted simultaneously. (B) Relative binding affinities (K_d values) of wild-type and mutant *saCodY* in the absence of GTP (purple) and the presence of GTP (green). The inset table indicates the binding constants (K_d values) of wild-type and mutant *saCodY* calculated by fitting a nonlinear regression curve (see also Supplementary Figure S7).

decreased, and CodY stops acting as a transcriptional repressor. Together, our EMSA data suggest that the GTP-binding site has an effect on CodY activation and that the interactions of CodY with GTP phosphates at the P-pocket have more influence on their activities.

Structural changes in the MBD, DBD and LHL after GTP binding

Two structures of the MBD of CodY have been reported by X-ray analysis (PDB entry: 2GX5- *bsCodY*_Apo, 2B18- *bsCodY* with Ile, respectively) (24,30). To investigate the structural changes resulting from the GTP binding of CodY, we compared the MBD, focusing on the Ile-binding site. No differences were observed in the MBD of CodY through the superposition of GTP-absent *bcCodY* with GTP-bound *saCodY*. *saCodY* and *bcCodY* exhibited folding similar to that seen in the structure of Ile-bound CodY (*bsCodY*_ILE; Supplementary Figure S8A). We did not detect any Ile molecules in the structure of *bcCodY*, but the Ile-binding site of the *bcCodY*_MBD was different from that of *bsCodY*_Apo (Supplementary Figure S8B and C). Residues associated with interactions with Ile, Y75 and T96 were in similar positions. E101, which is known to interact with the carbonyl group of Ile and form a salt bridge with R61, was on the opposite side as R61 in *bcCodY*. The position of R61 was also slightly different in *bcCodY* (Supplementary Figure S8C). It might have been difficult for E101 to hold R61 because of the deficiency in Ile. The structural distinction between MBD for the Ile-binding site was caused by the scarcity of Ile, but *bcCodY* appeared more similar to the

Ile-bound form than the Apo form. Thus, GTP binding was examined for comparison. The main difference in the MBD with GTP bound was the flipping of V22 in the loop between $\alpha 1$ and $\alpha 2$ (motif 1). The positions of other residues involved in GTP binding were similar (Supplementary Figure S8D). Moreover, when the DBDs were compared, there were no significant differences including in the HTH motif between *saCodY*, *bcCodY* and *bsCodY* (PDB entry: 2B0L) (Supplementary Figure S8E). We superimposed the MBDs of *saCodY* and *bcCodY* to inspect the changes induced by GTP in the LHL and DBD. The most striking structural change was that the LHL was bent by GTP binding. The superimposition of MBDs of *saCodY* (I), *bcCodY* and *saCodY* (II) showed dynamic movements of LHL and DBDs (Figure 5A). The DBD of each CodY bent at an angle of 15 degrees from the GTP-binding point (Figure 5B). The flexible LHL and DBD were fixed, and the side chain of E153 formed a hydrogen bond with GTP (Figure 3B). In addition, the DBD of *saCodY* (II) from a different dataset changed position, thus resulting in an angle of 13 degrees with *saCodY* (I) (Figure 5C). The DBDs of *saCodY* (II) and *bcCodY* made an angle of 6 degrees (Supplementary Figure S9). *saCodY* bound to DNA without GTP, but it was able to do so more efficiently (Figure 4) (15–20). By using the GTP molecule at a hinge site between LHL and MBD, CodY probably readjusts a flexible linker and thereby controls the positions of DBDs after sensing a GTP molecule. GTP may help CodY form a stable DNA-CodY complex by filling the GTP-binding pocket.

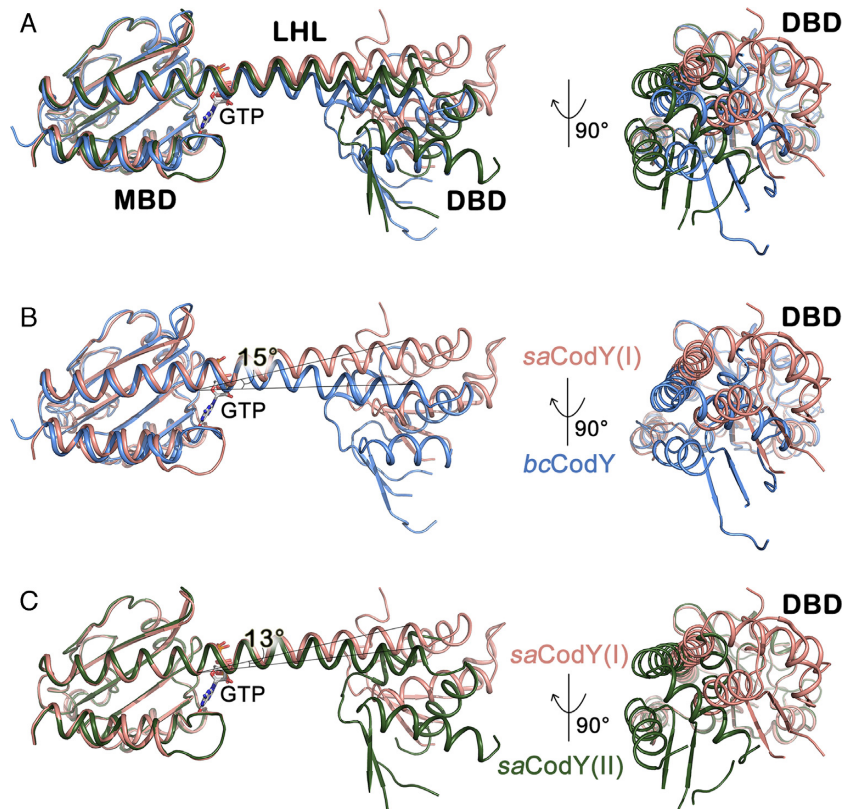


Figure 5. Molecular movements of DBD and LHL in two orientations. (A) The superimposition of the MBD from *saCodY* (I) (light pink), *bcCodY* (blue), and *saCodY* (II) (dark green) show the differences among the structural positions of the LHL and DBD. GTP is located at the point at which the LHL is bent. (B) The superimposition of the MBD from *saCodY* (I) and *bcCodY*. At this point, two LHLs, from *saCodY* (I) and *bcCodY*, are positioned at a 15° angle to each other. (C) The superimposition of the MBD from *saCodY* (I) and *saCodY* (II). Two LHLs, from *saCodY* (I) and *saCodY* (II), are positioned at a 13° angle to each other.

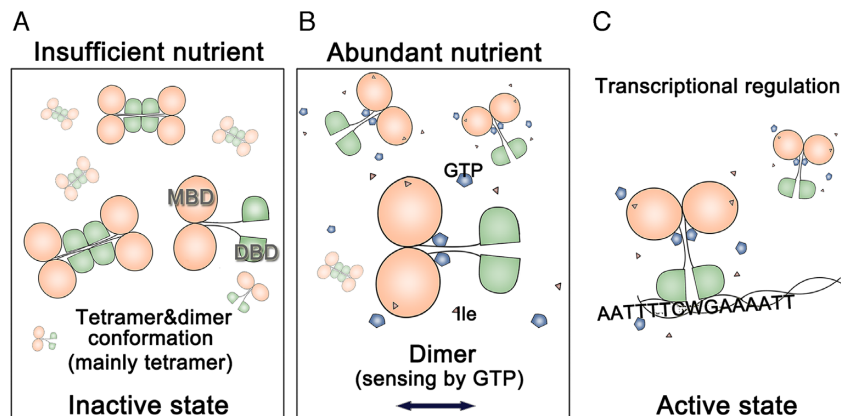


Figure 6. Proposed model of CodY state based on nutrient availability. (A) Under conditions with low nutrient availability (insufficient nutrition), CodY is in an inactive state. CodY exists mainly as tetramers but some exists as dimers. (B) In a nutrient-rich environment (abundant nutrition), ligand-bound CodY is rearranged as a dimer by sensing GTP, which makes CodY bind to DNA. (C) GTP-bound CodY is activated by binding DNA, and then regulates transcription. The labels 'MBD' and 'DBD' indicate MBD (orange) and DBD (green), respectively. The line connecting MBD and DBD represents LHL. The triangles labeled 'Ile' represent isoleucine molecules, and the purple pentagons labeled 'GTP' represent GTP molecules.

DISCUSSION

CodY responds to GTP and BCAA signals, and it regulates more than 100 genes that are primarily involved in bacterial environment adaptation in response to nutritional availability (1,10). In particular, GTP directly reflects the energy status of cells, and CodY senses the energy status and controls genes by directly binding GTP (15). The sensing of a particular nutrient may involve the direct binding of the molecule to its sensor or may occur via an indirect mechanism relying on the detection of a surrogate molecule that reflects nutrient abundance. Regardless of the manner in which nutrient sensing occurs, for a protein to be considered a sensor, its affinity must be within the range of the physiological fluctuations of the concentration of the nutrient or its surrogate (43). Despite the importance of a sensing mechanism, the GTP-bound CodY remains unknown. In this study, we report the first full-length CodY structure that has two different conformations, an inactive form and an intermediate form with two metabolites, GTP and Ile, which is ready to be activated, thus allowing DNA binding.

Interestingly, CodY of *Lactococcus lactis* (*l*CodY) and of *Streptococcus pneumoniae* (*sp*CodY) cannot respond to GTP (21,22). A structure-based sequence comparison of the GTP-binding sites in CodY analogs shows a possible structural basis for the inability of *l*CodY and *sp*CodY to bind GTP (Figure 3C). The common changes of *l*CodY and *sp*CodY are the substitution of three residues (F24, S43, and E153 in *sa*CodY) to tyrosine, asparagine, and glutamine, respectively (Figure 3C). Of particular note in the G-pocket is the change of glutamic acid (E153 in *sa*CodY), which hydrogen-bonds to the amino group of guanine, to glutamine, which has an uncharged side chain. In addition, the change of phenylalanine (F24 in *sa*CodY) to tyrosine may have an effect on the stacking interaction with the purine ring of GTP. The change of serine (S43 in *sa*CodY) in the P-pocket, which directly interacts with β -phosphate, to asparagine, which has a larger functional group than serine, may have a significant effect. In the SPR analysis, E153A and 3P5A were relevant to the G-pocket and P-pocket, respectively, and had a lower GTP-binding affinity than that of wild-type *sa*CodY (Supplementary Figures S5E and F, and S6). As a result, it seems reasonable to conclude that *l*CodY and *sp*CodY cannot bind to GTP, owing to the differences in the sequence of the GTP-binding site.

Branched-chain amino acids, particularly Ile, have an additive effect on the activation of CodY through direct interaction (11,16,27), and the dimerization interface of CodY is not substantially changed by this interaction (24,30). Our data also show that there are no significant differences in the Ile binding site between *bc*CodY and *sa*CodY. In its inactive form, CodY forms a tetramer, in which the HTH motif of the DBD is blocked by the MBDs of other protomers (Figures 1B and 2D). The sharing of the Ile-bound MBD presumably indicates that the MBD of *bc*CodY is the intermediate state after releasing Ile molecules. CodY mainly exists as a tetramer, but some is present as a dimer (Figure 2F and G). In a nutrient-deficient environment, CodY forms a tetramer, thereby preventing CodY from repressing transcription and acting as a roadblock (44). From the same point of view, *sa*CodY complexes with GTP and Ile in

a nutrient-rich environment. The CodY tetramer was separated into smaller units such as dimers or monomers by GTP, not Ile (Figure 2F–G, and Supplementary Figure S3A and B). Moreover, the DNA-binding affinity of CodY was improved by GTP binding (Figure 4). Ile also enhances the DNA-binding affinity of CodY, and GTP and BCAAs both have an additive effect, but they work independently (16). Together, these data suggest that CodY has different mechanisms of binding to these two metabolites even though CodY operates in the same ways using GTP and Ile as nutrient sensors.

From our results, we propose a model for CodY activation in response to nutrient signals, particularly GTP, as shown in Figure 6. The states of CodY are as follows. (A) The majority of CodY molecules form tetramers, but some exist as dimers in a harsh environment in which nutrient availability is low (inactive state). This structure prohibits CodY from binding to DNA and covering the HTH motif by using other protomers; consequently, genes normally repressed by CodY are activated. (B) The ligand-binding sites of CodY are nearly fully occupied when cells are in a nutrient-rich environment. CodY is rearranged into smaller units, such as dimers and monomers, by GTP, which enhances CodY's affinity for DNA. (C) The position of the DBD can be controlled via the modulation of the angle at the GTP-binding site or via the restraint of DBD mobility by GTP, thus increasing its DNA-binding ability (specifically, at promoters). CodY is activated and consequently regulates cellular metabolism (active state). However, conformational changes may occur after DNA binding.

CodY is a unique regulatory protein known as a pleiotropic repressor. How CodY is structurally able to detect a specific sequence and interact with various genes remains unclear. Further studies are required to identify the CodY-DNA complex to determine CodY's mechanism of action. Our results provide the first structure of full-length CodY and indicate that GTP plays a role in the ability of CodY to bind DNA. Structural data and EMSAs improved understanding of the role of GTP sensing in CodY's DNA-binding ability and its role as a pleiotropic transcription regulator.

ACCESSION NUMBERS

The atomic coordinates and structure factors have been deposited in Protein Data Bank, www.pdb.org with accession codes 5EY0, 5EY1, and 5EY2 for the *sa*CodY(I), *sa*CodY(II) and *bc*CodY, respectively.

SUPPLEMENTARY DATA

Supplementary Data are available at NAR Online.

ACKNOWLEDGEMENTS

We thank supporting staff of beamline BL1A of the Photon Factory (Tsukuba, Japan) and beamline 5C-SBII of Pohang Accelerator Light Source (Pohang, South Korea) for the help with data collection. The SPR instrument was provided by the Korea Basic Science Institute (Seoul, South Korea).

FUNDING

National Research Foundation of Korea [2013R1A1A2008404, M3A6A4044795, NCC1410671-3]; Korea University grants (to K.Y.H.). Funding for open access charge: National Research Foundation of Korea.

Conflict of interest statement. None declared.

REFERENCES

- Sonenshein, A.L. (2007) Control of key metabolic intersections in *Bacillus subtilis*. *Nat. Rev. Microbiol.*, **5**, 917–927.
- Buescher, J.M., Liebermeister, W., Jules, M., Uhr, M., Muntel, J., Botella, E., Hessling, B., Kleijn, R.J., Le Chat, L., Lecoq, F. *et al.* (2012) Global network reorganization during dynamic adaptations of *Bacillus subtilis* metabolism. *Science*, **335**, 1099–1103.
- Paul, L., Mishra, P.K., Blumenthal, R.M. and Matthews, R.G. (2007) Integration of regulatory signals through involvement of multiple global regulators: control of the *Escherichia coli* gltBDF operon by Lrp, IHF, Crp, and ArgR. *BMC Microbiol.*, **7**, 2.
- Gaal, T., Bartlett, M.S., Ross, W., Turnbough, C.L. Jr and Gourse, R.L. (1997) Transcription regulation by initiating NTP concentration: rRNA synthesis in bacteria. *Science*, **278**, 2092–2097.
- Lopez, J.M., Dromerick, A. and Freese, E. (1981) Response of guanosine 5'-triphosphate concentration to nutritional changes and its significance for *Bacillus subtilis* sporulation. *J. Bacteriol.*, **146**, 605–613.
- Boutte, C.C. and Crosson, S. (2013) Bacterial lifestyle shapes stringent response activation. *Trends Microbiol.*, **21**, 174–180.
- Traxler, M.F., Summers, S.M., Nguyen, H.T., Zacharia, V.M., Hightower, G.A., Smith, J.T. and Conway, T. (2008) The global, ppGpp-mediated stringent response to amino acid starvation in *Escherichia coli*. *Mol. Microbiol.*, **68**, 1128–1148.
- Serror, P. and Sonenshein, A.L. (1996) Interaction of CodY, a novel *Bacillus subtilis* DNA-binding protein, with the dpp promoter region. *Mol. Microbiol.*, **20**, 843–852.
- Molle, V., Nakaura, Y., Shivers, R.P., Yamaguchi, H., Losick, R., Fujita, Y. and Sonenshein, A.L. (2003) Additional targets of the *Bacillus subtilis* global regulator CodY identified by chromatin immunoprecipitation and genome-wide transcript analysis. *J. Bacteriol.*, **185**, 1911–1922.
- Sonenshein, A.L. (2005) CodY, a global regulator of stationary phase and virulence in Gram-positive bacteria. *Curr. Opin. Microbiol.*, **8**, 203–207.
- Pohl, K., Francois, P., Stenz, L., Schlink, F., Geiger, T., Herbert, S., Goerke, C., Schrenzel, J. and Wolz, C. (2009) CodY in *Staphylococcus aureus*: a regulatory link between metabolism and virulence gene expression. *J. Bacteriol.*, **191**, 2953–2963.
- Brinsmade, S.R., Alexander, E.L., Livny, J., Stettner, A.I., Segre, D., Rhee, K.Y. and Sonenshein, A.L. (2014) Hierarchical expression of genes controlled by the *Bacillus subtilis* global regulatory protein CodY. *Proc. Natl. Acad. Sci. U.S.A.*, **111**, 8227–8232.
- Belitsky, B.R. and Sonenshein, A.L. (2013) Genome-wide identification of *Bacillus subtilis* CodY-binding sites at single-nucleotide resolution. *Proc. Natl. Acad. Sci. U.S.A.*, **110**, 7026–7031.
- Stenz, L., Francois, P., Whiteson, K., Wolz, C., Linder, P. and Schrenzel, J. (2011) The CodY pleiotropic repressor controls virulence in gram-positive pathogens. *FEMS Immunol. Med. Microbiol.*, **62**, 123–139.
- Ratnayake-Lecamwasam, M., Serror, P., Wong, K.W. and Sonenshein, A.L. (2001) *Bacillus subtilis* CodY represses early-stationary-phase genes by sensing GTP levels. *Genes Dev.*, **15**, 1093–1103.
- Shivers, R.P. and Sonenshein, A.L. (2004) Activation of the *Bacillus subtilis* global regulator CodY by direct interaction with branched-chain amino acids. *Mol. Microbiol.*, **53**, 599–611.
- Handke, L.D., Shivers, R.P. and Sonenshein, A.L. (2008) Interaction of *Bacillus subtilis* CodY with GTP. *J. Bacteriol.*, **190**, 798–806.
- Bennett, H.J., Pearce, D.M., Glenn, S., Taylor, C.M., Kuhn, M., Sonenshein, A.L., Andrew, P.W. and Roberts, I.S. (2007) Characterization of *relA* and *codY* mutants of *Listeria monocytogenes*: identification of the CodY regulon and its role in virulence. *Mol. Microbiol.*, **63**, 1453–1467.
- Dineen, S.S., Villapakkam, A.C., Nordman, J.T. and Sonenshein, A.L. (2007) Repression of *Clostridium difficile* toxin gene expression by CodY. *Mol. Microbiol.*, **66**, 206–219.
- Majerczyk, C.D., Sadykov, M.R., Luong, T.T., Lee, C., Somerville, G.A. and Sonenshein, A.L. (2008) *Staphylococcus aureus* CodY negatively regulates virulence gene expression. *J. Bacteriol.*, **190**, 2257–2265.
- Hendriksen, W.T., Bootsma, H.J., Esteveo, S., Hoogenboezem, T., de Jong, A., de Groot, R., Kuipers, O.P. and Hermans, P.W. (2008) CodY of *Streptococcus pneumoniae*: link between nutritional gene regulation and colonization. *J. Bacteriol.*, **190**, 590–601.
- Petrancovic, D., Guedon, E., Sperandio, B., Delorme, C., Ehrlich, D. and Renault, P. (2004) Intracellular effectors regulating the activity of the *Lactococcus lactis* CodY pleiotropic transcription regulator. *Mol. Microbiol.*, **53**, 613–621.
- Villapakkam, A.C., Handke, L.D., Belitsky, B.R., Levnikov, V.M., Wilkinson, A.J. and Sonenshein, A.L. (2009) Genetic and biochemical analysis of the interaction of *Bacillus subtilis* CodY with branched-chain amino acids. *J. Bacteriol.*, **191**, 6865–6876.
- Levnikov, V.M., Blagova, E., Colledge, V.L., Lebedev, A.A., Williamson, D.C., Sonenshein, A.L. and Wilkinson, A.J. (2009) Structural rearrangement accompanying ligand binding in the GAF domain of CodY from *Bacillus subtilis*. *J. Mol. Biol.*, **390**, 1007–1018.
- Brinsmade, S.R., Kleijn, R.J., Sauer, U. and Sonenshein, A.L. (2010) Regulation of CodY activity through modulation of intracellular branched-chain amino acid pools. *J. Bacteriol.*, **192**, 6357–6368.
- Brinsmade, S.R. and Sonenshein, A.L. (2011) Dissecting complex metabolic integration provides direct genetic evidence for CodY activation by guanine nucleotides. *J. Bacteriol.*, **193**, 5637–5648.
- Guédon, E., Sperandio, B., Pons, N., Ehrlich, S.D. and Renault, P. (2005) Overall control of nitrogen metabolism in *Lactococcus lactis* by CodY, and possible models for CodY regulation in Firmicutes. *Microbiology*, **151**, 3895–3909.
- den Hengst, C.D., van Hijum, S.A., Geurts, J.M., Nauta, A., Kok, J. and Kuipers, O.P. (2005) The *Lactococcus lactis* CodY regulon: identification of a conserved cis-regulatory element. *J. Biol. Chem.*, **280**, 34332–34342.
- Belitsky, B.R. and Sonenshein, A.L. (2008) Genetic and biochemical analysis of CodY-binding sites in *Bacillus subtilis*. *J. Bacteriol.*, **190**, 1224–1236.
- Levnikov, V.M., Blagova, E., Joseph, P., Sonenshein, A.L. and Wilkinson, A.J. (2006) The structure of CodY, a GTP- and isoleucine-responsive regulator of stationary phase and virulence in gram-positive bacteria. *J. Biol. Chem.*, **281**, 11366–11373.
- Otwinowski, Z. and Minor, W. (1997) In: Carter, C.W. Jr (ed). *Methods in Enzymology*. Academic Press, Vol. **276**, pp. 307–326.
- Vagin, A. and Teplyakov, A. (1997) MOLREP: an automated program for molecular replacement. *J. Appl. Crystallogr.*, **30**, 1022–1025.
- Collaborative Computational Project, N. (1994) The CCP4 suite: programs for protein crystallography. *Acta Crystallogr. D: Biol. Crystallogr.*, **50**, 760–763.
- McCoy, A.J., Grosse-Kunstleve, R.W., Adams, P.D., Winn, M.D., Storoni, L.C. and Read, R.J. (2007) Phaser crystallographic software. *J. Appl. Crystallogr.*, **40**, 658–674.
- Adams, P.D., Afonine, P.V., Bunkoczi, G., Chen, V.B., Davis, I.W., Echols, N., Headd, J.J., Hung, L.-W., Kapral, G.J., Grosse-Kunstleve, R.W. *et al.* (2010) PHENIX: a comprehensive Python-based system for macromolecular structure solution. *Acta Crystallogr. D*, **66**, 213–221.
- Terwilliger, T.C., Adams, P.D., Read, R.J., McCoy, A.J., Moriarty, N.W., Grosse-Kunstleve, R.W., Afonine, P.V., Zwart, P.H. and Hung, L.-W. (2009) Decision-making in structure solution using Bayesian estimates of map quality: the PHENIX AutoSol wizard. *Acta Crystallogr. D: Biol. Crystallogr.*, **65**, 582–601.
- Terwilliger, T.C., Grosse-Kunstleve, R.W., Afonine, P.V., Moriarty, N.W., Zwart, P.H., Hung, L.-W., Read, R.J. and Adams, P.D. (2008) Iterative model building, structure refinement and density modification with the PHENIX AutoBuild wizard. *Acta Crystallogr. D*, **64**, 61–69.
- Emsley, P. and Cowtan, K. (2004) Coot: model-building tools for molecular graphics. *Acta Crystallogr. D: Biol. Crystallogr.*, **60**, 2126–2132.

39. Murshudov, G.N., Skubak, P., Lebedev, A.A., Pannu, N.S., Steiner, R.A., Nicholls, R.A., Winn, M.D., Long, F. and Vagin, A.A. (2011) REFMAC5 for the refinement of macromolecular crystal structures. *Acta Crystallogr. D: Biol. Crystallogr.*, **67**, 355–367.
40. Davis, I.W., Murray, L.W., Richardson, J.S. and Richardson, D.C. (2004) MOLPROBITY: structure validation and all-atom contact analysis for nucleic acids and their complexes. *Nucleic Acids Res.*, **32**, W615–W619.
41. Blagova, E.V., Levnikov, V.M., Tachikawa, K., Sonenshein, A.L. and Wilkinson, A.J. (2003) Crystallization of the GTP-dependent transcriptional regulator CodY from *Bacillus subtilis*. *Acta Crystallogr. D, Biol. Crystallogr.*, **59**, 155–157.
42. Joseph, P., Ratnayake-Lecamwasam, M. and Sonenshein, A.L. (2005) A region of *Bacillus subtilis* CodY protein required for interaction with DNA. *J. Bacteriol.*, **187**, 4127–4139.
43. Efeyan, A., Comb, W.C. and Sabatini, D.M. (2015) Nutrient-sensing mechanisms and pathways. *Nature*, **517**, 302–310.
44. Belitsky, B.R. and Sonenshein, A.L. (2011) Roadblock repression of transcription by *Bacillus subtilis* CodY. *J. Mol. Biol.*, **411**, 729–743.